THE JOURNAL OF PHYSICAL CHEMISTRY A

 VOLUME 111, NUMBER 8, MARCH 1, 2007

# ARTICLES

## Phosphorescent Resonant Energy Transfer between Iridium Complexes

**Dorothee Wasserberg, Stefan C. J. Meskers, and René A. J. Janssen***

*Molecular Materials and Nanosystems, Eindhoven University of Technology, P.O. Box 513, 5600 MB Eindhoven, The Netherlands*

*Received: September 16, 2006; In Final Form: January 5, 2007*

The mechanism for triplet energy transfer from the green-emitting *fac*-tris[2-(4′-*tert*-butylphenyl)pyridinato]-iridium (Ir(*t*Bu-ppy)$_3$) complex to the red-emitting bis[2-(2′-benzothienyl)pyridinato-*N*,*C*$^{3'}$)(acetylacetonato)-iridium (Ir(btp)$_2$(acac)) phosphor has been investigated using steady-state and time-resolved photoluminescence spectroscopy. [2,2′;5,′2″]Terthiophene (3T) was also used as triplet energy acceptor to differentiate between the two common mechanisms for energy transfer, i.e., the direct exchange of electrons (Dexter transfer) or the coupling of transition dipoles (Förster transfer). Unlike Ir(btp)$_2$(acac), 3T can only be active in Dexter energy transfer because it has a negligible ground state absorption to the $^3(\pi-\pi^*)$ state. The experiments demonstrate that in semidilute solution, the $^3$MLCT state of Ir(*t*Bu-ppy)$_3$ can transfer its triplet energy to the lower-lying $^3(\pi-\pi^*)$ states of both Ir(btp)$_2$(acac) and 3T. For both acceptors, this transfer occurs via a diffusion-controlled reaction with a common rate constant ($k_{en} = 3.8 \times 10^9$ L mol$^{-1}$ s$^{-1}$). In a solid-state polymer matrix, the two acceptors, however, show entirely different behavior. The $^3$MLCT phosphorescence of Ir(*t*Bu-ppy)$_3$ is strongly quenched by Ir(btp)$_2$(acac) but not by 3T. This reveals that under conditions where molecular diffusion is inhibited, triplet energy transfer only occurs via the Förster mechanism, provided that the transition dipole moments involved on energy donor and acceptor are not negligible. With the use of the Förster radius for triplet energy transfer from Ir(*t*Bu-ppy)$_3$ to Ir(btp)$_2$(acac) of $R_0 = 3.02$ nm, the experimentally observed quenching is found to agree quantitatively with a model for Förster energy transfer that assumes a random distribution of acceptors in a rigid matrix.

### Introduction

Organic and polymeric light-emitting diodes attract considerable attention for applications in multicolor displays and lighting applications. In OLEDs and PLEDs visible light is generated via radiative decay of excited states formed by the recombination of the holes and electrons injected into the organic semiconductor.[1−3] Spin statistics favor formation of triplet over singlet excited states, which poses a limitation to the internal quantum efficiency of LEDs based on fluorescent small molecules or polymers. By using phosphorescent emitters in the active layer it is possible to capture both singlet and triplet excited states and increase the internal quantum efficiency.[4,5]

In recent years considerable progress in electrophosphorescent LEDs has been achieved by using organometallic (e.g., Pt, Ir) complexes as dopants in small organic molecule[6−9] and polymer hosts.[10−15] The large spin−orbit coupling associated with platinum and iridium causes the triplet metal-to-ligand charge-transfer $^3$MLCT and ligand-based $^3(\pi-\pi^*)$ states of the phosphors to couple radiatively to the ground state and achieve internal quantum efficiencies approaching 100% in OLEDs.[16]

Transfer of excited-state energy plays a crucial role in the operation of these electrophosphorescent devices. In many

* Corresponding author. E-mail: r.a.j.janssen@tue.nl.

10.1021/jp066055q CCC: $37.00 
Published on Web 02/06/2007

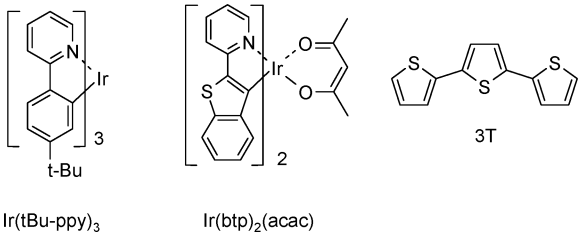


$Ir(tBu\text{-}ppy)_3$ $Ir(btp)_2(acac)$

**Figure 1.** Structures of the green-emitting Ir(*t*Bu-ppy)$_3$ phosphor, the red-emitting Ir(btp)$_2$(acac) phosphor, and the low-triplet-energy 3T molecule.

systems singlet and triplet excitons are first generated by electron−hole recombination in the organic or polymer host and then transfer their energy to the dopant. Alternatively, the triplet state of the phosphorescent dye may be formed by charge transfer from the host or nearby injection layers. In either case, the singlet and triplet energy levels of the host have to be well above the triplet state of the emitter to be efficient and prevent back transfer. The actual transfer of excited-state energy can occur via different mechanisms. Dexter energy transfer involves the actual exchange of electrons between donor and acceptor and only occurs when their molecular orbitals overlap. Hence, the efficiency of Dexter energy transfer drops exponentially with distance. The Förster mechanism, on the other hand, relies on coupling of transition dipole moments to transfer energy and can operate over longer distances up to several nanometers. An important difference between the two mechanisms is that the oscillator strengths of the optical transitions on the donor and acceptor are crucial for Förster energy transfer but have no influence on the rate of Dexter energy transfer.

While the mechanism of energy transfer between host and dopant has received considerable interest,[17−22] less attention has been given to the mechanism of energy transfer between (different) dopants in the host. Such processes may be important for the development white-light LEDs.[23−28] Intriguing experiments regarding excited-state energy transfer between two dopants have been described by Forrest and co-workers on the Förster transfer from a green-emitting phosphor (Ir(ppy)$_3$) to a red-emitting fluorescent dye (DCM2),[29,30] where phosphor sensitization was used to increase the internal quantum efficiency of fluorescent OLEDs. Energy transfer between phosphorescent dopants has also been used in OLEDs comprising a wide energy gap host layer with three different iridium dyes that emit blue, green, and red light, respectively.[31] With the use of time-resolved photoluminescence it was shown that energy transfer occurs from the blue phosphor to the green and red phosphors, but not from the green to red because the latter were used in low concentrations.[31] More recently, Förster triplet energy transfer was considered as the mechanism that is responsible for the concentration quenching of phosphorescent emission.[32]

We investigated the mechanism of triplet energy transfer in semidilute solution and in a rigid polymer host matrix from the green-emitting Ir(*t*Bu-ppy)$_3$ to the red-emitting Ir(btp)$_2$(acac) dye (Figure 1) using steady-state and time-resolved photoluminescence. The results are compared to triplet energy transfer from Ir(*t*Bu-ppy)$_3$ to 3T (Figure 1). Unlike Ir(btp)$_2$(acac), 3T cannot accept triplet energy via Förster transfer because it has a negligible $T_1 \leftarrow S_0$ absorption. Hence, triplet energy transfer to 3T must involve the Dexter mechanism. We find that in semidilute solution triplet energy transfer occurs to both Ir(btp)$_2$(acac) and 3T via a diffusion-controlled reaction. In a rigid matrix, however, where molecular diffusion is absent, only Ir(btp)$_2$(acac) quenches the Ir(*t*Bu-ppy)$_3$ phosphorescence. This difference suggests that phosphorescent resonance energy transfer in the solid state occurs predominantly via the Förster mechanism.

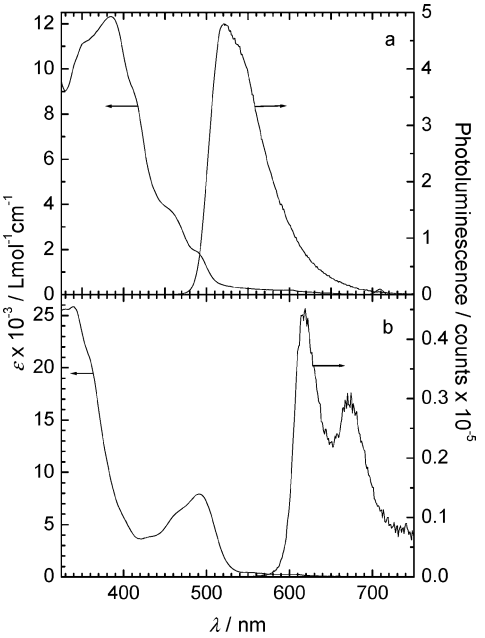


**Figure 2.** Molar absorption coefficient ($\epsilon$) and photoluminescence spectra of (a) Ir(*t*Bu-ppy)$_3$ in chlorobenzene solution (10 $\mu$M) and (b) Ir(btp)$_2$(acac) in chlorobenzene solution (185 $\mu$M). The photoluminescence was recorded under inert atmosphere using an excitation wavelength of 400 nm.

## Results and Discussion

**Energy Transfer between Ir(*t*Bu-ppy)$_3$ and Ir(btp)$_2$(acac) in Solution.** The absorption spectrum of Ir(*t*Bu-ppy)$_3$ in chlorobenzene solution recorded at room temperature shows a strong band at 380 nm ($\epsilon \sim 12000$ L mol$^{-1}$ cm$^{-1}$) that is attributed to a spin-allowed metal-to-ligand charge-transfer ($^1$MLCT) transition (Figure 2a).[33] The two weaker bands at 460 and 490 nm are assigned to spin-forbidden $^3$MLCT transitions. The strong spin−orbit coupling of $Ir^{3+}$ causes these transitions to mix with higher-lying spin-allowed transitions and acquire appreciable intensity. The photoluminescence of Ir(*t*Bu-ppy)$_3$ originates from lowest energy $^3$MLCT transition and shows a maximum at 515 nm (2.41 eV) (Figure 2).[34,35] The photoluminescence spectrum shows little or no vibronic structure. In deoxygenated chlorobenzene solution the photoluminescence quantum yield for Ir(*t*Bu-ppy)$_3$ is $\phi = 0.56 \pm 0.04$ when referenced to *N*,*N*′-bis(1-ethylpropyl)perylenediimide ($\phi = 1$). For the closely related Ir(ppy)$_3$ complex, $\phi = 0.40 \pm 0.1$ has been reported in deoxygenated toluene solution[36] and $\phi = 0.97 \pm 0.02$ in a solid-state host matrix at 1.5 mol % concentration.[37]

The room temperature absorption spectrum of Ir(btp)$_2$(acac) in chlorobenzene exhibits a band at 491 nm (2.52 eV; $\epsilon \sim 8000$ L mol$^{-1}$ cm$^{-1}$) (Figure 2b) that has been assigned to the $^3$MLCT state.[38] The photoluminescence of Ir(btp)$_2$(acac) has a maximum at 620 nm (2.00 eV) with vibronic bands at 670 and 740 nm. The large Stokes shift of ~129 nm (0.52 eV) is due to the fact that the emission of Ir(btp)$_2$(acac) does not occur from the $^3$MLCT state but originates predominantly from the btp ligand-based $^3(\pi-\pi^*)$ state.[38] The photoluminescence quantum yield of Ir(btp)$_2$(acac) in MeTHF solution is $\phi = 0.21$[38] and $\phi = 0.51 \pm 0.01$ in a solid-state host matrix at 1.4 mol % concentration.[37]

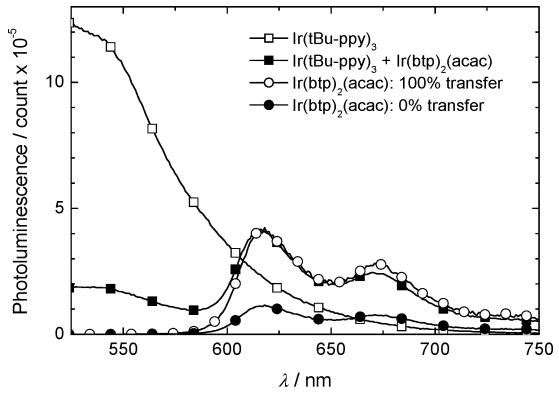


**Figure 3.** Photoluminescence spectra of Ir(*t*Bu-ppy)$_3$ (10 mM) (open squares) and of a mixture of Ir(*t*Bu-ppy)$_3$ (10 mM) and Ir(btp)$_2$(acac) (550 $\mu$M) (solid squares) in chlorobenzene. The photoluminescence spectra were recorded under inert atmosphere at room temperature using an excitation wavelength of 500 nm. For comparison, the expected photoluminescence intensity of Ir(btp)$_2$(acac) in the mixture is shown for two limiting cases (first) assuming that no energy transfer occurs (solid circles) and (second) assuming 100% energy transfer (open circles). See ref 40.

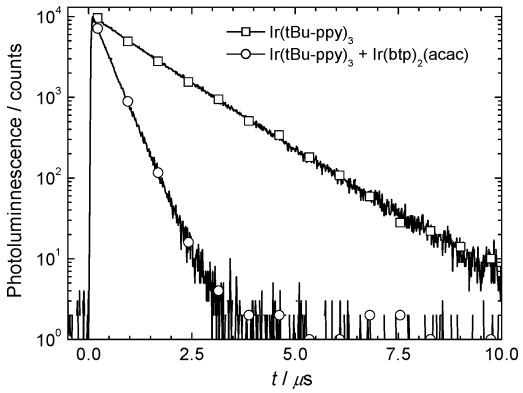


**Figure 4.** Time-resolved photoluminescence recorded at 535 nm of Ir(*t*Bu-ppy)$_3$ in chlorobenzene (10 mM) (squares) and of Ir(*t*Bu-ppy)$_3$ (10 mM) mixed with Ir(btp)$_2$(acac) (550 $\mu$M) (circles). The photoluminescence was recorded under inert atmosphere at room temperature with pulsed excitation at 400 nm.

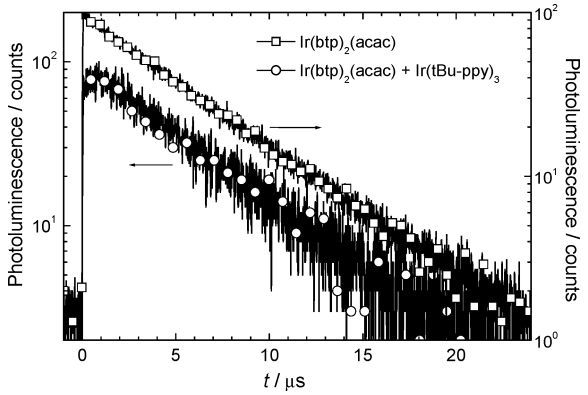


**Figure 5.** Time-resolved photoluminescence recorded at 680 nm of Ir(btp)$_2$(acac) (550 $\mu$M) in chlorobenzene (squares) and of Ir(btp)$_2$(acac) (550 $\mu$M) mixed with Ir(*t*Bu-ppy)$_3$ (10 mM) (circles). The photoluminescence was recorded under inert atmosphere at room temperature with pulsed excitation at 400 nm.

The different nature of lowest energy triplet excited states of Ir(*t*Bu-ppy)$_3$ [$^3$MLCT] and Ir(btp)$_2$(acac) [$^3(\pi-\pi^*)$] is supported by the difference in vibrational structure of the two photoluminescence spectra. Luminescence from a $^3$MLCT state generally gives rise to a broad, featureless band, while that of $^3(\pi-\pi^*)$ states can be highly structured, featuring the vibrational modes of the ground state ligand that couple to the transition.[38,39]

The $^3$MLCT photoluminescence of Ir(*t*Bu-ppy)$_3$ and the $^3$MLCT absorption spectrum of Ir(btp)$_2$(acac) overlap in the region between 500 and 550 nm. Hence, energy transfer from the triplet state of Ir(*t*Bu-ppy)$_3$ to Ir(btp)$_2$(acac) is energetically possible. To investigate the occurrence of resonant energy transfer between the two phosphorescent emitters, the photoluminescence spectrum of a mixed solution of the two dyes was recorded. Figure 3. reveals that the emission of Ir(*t*Bu-ppy)$_3$ at 535 nm is significantly quenched (quenching factor, $Q = 6.5$) after addition of Ir(btp)$_2$(acac). At the same time, the photoluminescence at 620 nm of Ir(btp)$_2$(acac) increases significantly.[40] The spectra demonstrate that triplet energy transfer occurs from the $^3$MLCT state of Ir(*t*Bu-ppy)$_3$ to the $^3(\pi-\pi^*)$ state of Ir(btp)$_2$(acac). On the basis of the steady-state photoluminescence spectra it is difficult to quantify the results because the spectra have been recorded in front face geometry, which introduces some uncertainty in collecting the luminescent light. For comparison, Figure 3 also shows the photoluminescence spectra of Ir(btp)$_2$(acac) for two limiting cases: (first) assuming that the emission only occurs from photons directly absorbed by Ir(btp)$_2$(acac) (solid circles) and (second) assuming the red emission occurs from photons absorbed by Ir(btp)$_2$(acac) and Ir(*t*Bu-ppy)$_3$ (open circles). The experimental spectrum of the mix (solid squares) closely follows the latter curve within the wavelength range of Ir(btp)$_2$(acac) emission. This suggests that the energy transfer is nearly complete. The 15% residual emission of Ir(*t*Bu-ppy)$_3$ at 535 nm, however, shows that it is not quantitative under these conditions.

To quantify the triplet energy transfer and determine the rate constants for the process, time-resolved single-photon counting experiments were performed (Figures 4 and 5).

The lifetime of Ir(*t*Bu-ppy)$_3$ is reduced from 1.30 $\mu$s to 345 ns upon addition of 550 $\mu$M Ir(btp)$_2$(acac) (Figure 4, Table 1) when excited at 400 nm. The pseudo-first-order rate constant for quenching via energy transfer rate under these conditions can be calculated from the lifetimes in presence ($\tau_Q$) and absence ($\tau_0$) of the Ir(btp)$_2$(acac) quencher via $k_q = \tau_Q^{-1} - \tau_0^{-1} = 2.1 \times 10^6$ s$^{-1}$. Assuming that the quenching is proportional to the concentration of the Ir(btp)$_2$(acac) quencher (550 $\mu$M), the second-order rate constant for energy transfer is $k_{en} = k_q/[Q] = 3.8 \times 10^9$ L mol$^{-1}$ s$^{-1}$.

The sub-microsecond rate for energy transfer inferred from the photoluminescence quenching of the Ir(*t*Bu-ppy)$_3$ can also be observed as a slow increase of the emission of Ir(btp)$_2$(acac). Figure 5 shows the time-resolved photoluminescence at 680 nm of Ir(btp)$_2$(acac) in solution, before and after mixing with Ir(*t*Bu-ppy)$_3$. While the decay kinetics of the two Ir(btp)$_2$(acac) emission traces are very similar with a lifetime of 5.4 $\mu$s, the rise of the two signals is distinctly different. For the pure Ir(btp)$_2$(acac) dye the maximum emission coincides with the end of the excitation pulse, but in the mixed solution there is an additional slow rise component with a time constant of 410 ns (Figure 5). This rise time is similar to the time constant of $k_q^{-1} = 476$ ns for quenching via energy transfer determined from the lifetime reduction of Ir(*t*Bu-ppy)$_3$ (Table 1).

The correspondence between the time constants for the rise of the emission of Ir(btp)$_2$(acac) and the quenching of Ir(*t*Bu-ppy)$_3$ in the mixed solution strongly suggests that the two processes are related, consistent with a triplet energy transfer reaction. It is of interest to note that the second-order rate constant for the quenching ($k_{en} = 3.8 \times 10^9$ L mol$^{-1}$ s$^{-1}$) is of the same order of magnitude as the rate constant for diffusional

**TABLE 1: Photoluminescence Lifetimes Recorded of the Pure Iridium Dyes and in Mixtures with Quenchers Determined in Solution and in a PS Matrix**

| sample | dye | quencher | $\lambda$ (nm) | $\tau_1$ (ns) | $\tau_2$ (ns) | [dye] (mM) | [Q] (mM) |
|---|---|---|---|---|---|---|---|
| chloro-benzene | Ir(*t*Bu-ppy)$_3$ | | 535 | 1300[a] | | 10 | |
| | Ir(btp)$_2$(acac) | | 680 | 5400 | | 0.55 | |
| | Ir(*t*Bu-ppy)$_3$ | Ir(btp)$_2$ (acac) | 535 | 345 | | 10 | 0.55 |
| | Ir(*t*Bu-ppy)$_3$ | Ir(btp)$_2$ (acac) | 680 | *412*[b] | 5430 | 10 | 0.55 |
| PS film | Ir(*t*Bu-ppy)$_3$ | | 535 | 2510[c] | | 90 | |
| | Ir(btp)$_2$(acac) | | 680 | 5490 | | 100 | |
| | Ir(*t*Bu-ppy)$_3$ | Ir(btp)$_2$ (acac) | 535 | 39 | 248 | 90 | 90 |
| | Ir(*t*Bu-ppy)$_3$ | Ir(btp)$_2$ (acac) | 680 | *51*[b] | 5690 | 90 | 90 |
| MeTHF | Ir(*t*Bu-ppy)$_3$ | | 535 | 1730[a] | | 1 | |
| | Ir(*t*Bu-ppy)$_3$ | 3T | 535 | 217 | | 1 | 1 |
| PS film (80 K) | Ir(*t*Bu-ppy)$_3$ | | 535 | 2070[c] | | 100 | |
| | Ir(*t*Bu-ppy)$_3$ | 3T | 535 | 1910 | | 100 | 210 |

[a] The increased lifetime of Ir(*t*Bu-ppy)$_3$ in MeTHF compared to that in chlorobenzene is partly due to the lower refractive index (1.408 vs 1.524) that causes a slower radiative decay ($\tau \sim n^{-2}$) and possibly due to less triplet−triplet annihilation at the 10-fold lower concentration used. [b] Lifetimes in italics refer to a rise-time component. [c] The two entries labeled with "*c*" differ due to sample-to-sample variations.

collision $k_{diff} = 8.7 \times 10^9$ L mol$^{-1}$ s$^{-1}$ in chlorobenzene derived from the Debye equation ($k_{diff} = 8000RT/3\eta$)[41] and the viscosity $\eta = 0.758 \times 10^{-3}$ Pa·s of chlorobenzene at 298 K.[42] Hence, the energy transfer reaction in solution is, to a large extent, diffusion controlled. Both Dexter and Förster energy transfer strongly depend on the distance between donor and acceptor, and without further experimental data it is not possible to distinguish between these two mechanisms. To resolve this issue, energy transfer is studied in a rigid matrix.

**Energy Transfer between Ir(*t*Bu-ppy)$_3$ and Ir(btp)$_2$(acac) in Thin Films.** To further investigate the mechanism of energy transfer, the Ir(*t*Bu-ppy)$_3$ and Ir(btp)$_2$(acac) emitters were mixed in polystyrene (PS). After dissolving the components in chlorobenzene, thin PS films were made by spin coating on quartz substrates. Immobilized in the PS matrix and cooled to 80 K, energy transfer between the two dyes via molecular diffusion is improbable and energy transfer over longer distances can only be the result of a Förster energy transfer.

Figure 6 shows the photoluminescence spectra of Ir(*t*Bu-ppy)$_3$ and Ir(btp)$_2$(acac), together with that of a mixture of the two dyes dispersed in the PS matrix. The spectra show that the photoluminescence quenching of Ir(*t*Bu-ppy)$_3$ by Ir(btp)$_2$(acac) is very significant under these conditions and more efficient than in solution. The photoluminescence intensity at 535 nm of Ir(*t*Bu-ppy)$_3$ is strongly quenched ($Q = 62$). Simultaneously, the photoluminescence intensity of Ir(btp)$_2$(acac) increases 5-fold in the mixed film. This is actually larger than the 2.5-fold increase which is estimated for 100% energy transfer by considering the number of absorbed photons in the mixed film and in the film containing only Ir(btp)$_2$(acac). These estimates were obtained from the molar absorption coefficients of the two dyes at the excitation wavelength (400 nm), their molar concentrations in the PS film, and the film thickness as measured with a profilometer. The deviation is ascribed to unavoidable differences in measurement conditions related to the alignment of sample and cryostat.

The triplet energy transfer inferred from the photoluminescence spectra is supported by the time-resolved luminescence data recorded at 535 nm. The lifetime of the Ir(*t*Bu-ppy)$_3$

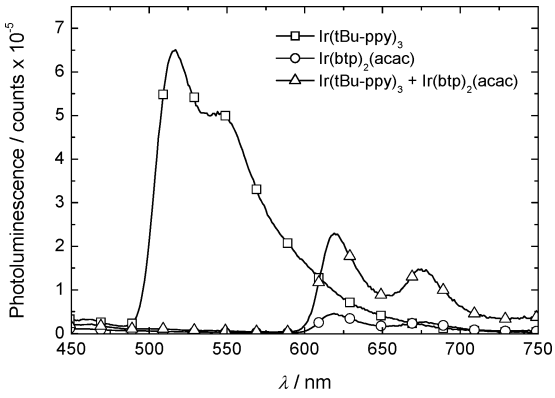


**Figure 6.** Photoluminescence spectra of PS films blended with 7 wt % (90 mM) Ir(*t*Bu-ppy)$_3$ (squares), 7 wt % (100 mM) Ir(btp)$_2$(acac) (circles), and a composite of 7 wt % (90 mM) Ir(*t*Bu-ppy)$_3$ and 6 wt % (90 mM) Ir(btp)$_2$(acac) (triangles). The spectra were recorded at 80 K using an excitation wavelength of 400 nm recorded under inert atmosphere.

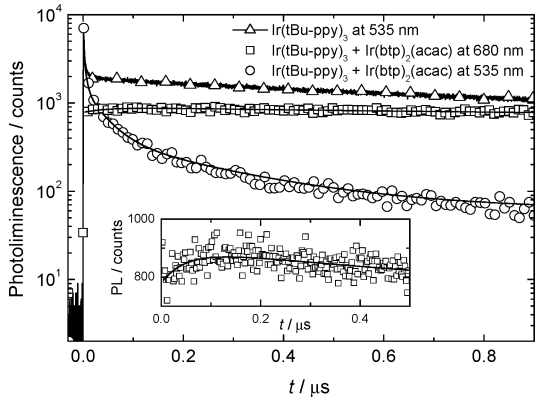


**Figure 7.** Time-resolved photoluminescence of PS films containing 7 wt % (90 mM) Ir(*t*Bu-ppy)$_3$ recorded at 535 nm (up triangles) and containing a mix of 7 wt % (90 mM) Ir(*t*Bu-ppy)$_3$ and 6 wt % (90 mM) Ir(btp)$_2$(acac) recorded at 535 nm (circles) and 680 nm (squares). The photoluminescence was recorded under inert atmosphere at 80 K with pulsed excitation at 400 nm. The solid lines are fits to the data for the mixture. The inset shows an expansion of the data in a linear plot.

emission is significantly reduced after mixing it with Ir(btp)$_2$(acac), while that of the Ir(btp)$_2$(acac) itself does not change significantly upon mixing (Figure 7, and Table 1). In the mixture of the two emitters, three lifetime components (4.9, 39, and 248 ns) describe the decay of the emission at 535 nm, corresponding to Ir(*t*Bu-ppy)$_3$ (Table 1). It should be noted that none of these components corresponds to the photoluminescence lifetime of the pure Ir(*t*Bu-ppy)$_3$ dye (2.51 $\mu$s), suggesting that the excited state of Ir(*t*Bu-ppy)$_3$ is effectively quenched in the mixed film. The shortest lifetime component (4.9 ns) arises from scattering of the excitation beam through the single monochromator of the setup and is neglected. The two other time constants, represent a fast (39 ns, relative amplitude 1.0) and a slower (248 ns, relative amplitude 0.34) energy transfer process. The occurrence of multiple lifetimes for the energy transfer, instead of one, is probably due to the dispersion of distances within the solid phase. From the shorter time constant ($\tau = 39$ ns; $k_{decay} = 2.56 \times 10^7$ s$^{-1}$) and the lifetime $\tau_0 = 2.51$ $\mu$s of pure Ir(*t*Bu-ppy)$_3$ in PS, a quenching factor of $Q = \tau_0/\tau - 1 = 63$ is predicted, in good agreement with the value $Q = 62$ obtained from the photoluminescence intensity (Figure 6). This demonstrates the quantitative agreement of the steady-state and time-resolved photoluminescence data. The rate constant for quench-

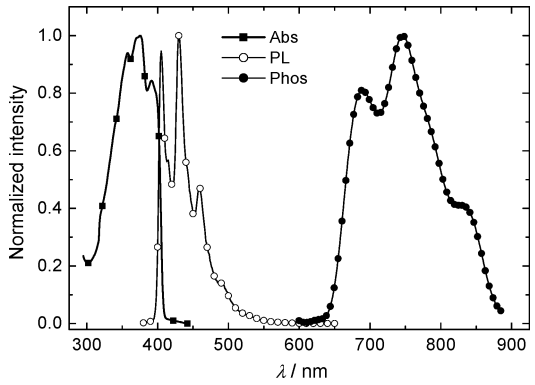


**Figure 8.** Normalized absorption, steady-state fluorescence, and gated phosphorescence spectra of 3T in MeTHF at 80 K. Phosphorescence spectra were recorded with gated detection during 2 ms at 200 ns of delay time after excitation. Excitation at 370 nm. From the 0−0 transitions in the fluorescence (405 nm) and phosphorescence spectra (689 nm), the $S_1$ and $T_1$ energies have been determined at 3.06 and 1.80 eV.

ing via energy transfer under these conditions is $k_q = \tau_Q^{-1} - \tau_0^{-1} = 2.52 \times 10^7\ s^{-1}$.

Similar to the mixed solutions, the rise of the emission of $Ir(btp)_2(acac)$ in the PS film with the mixed dyes is much slower than for the pure $Ir(btp)_2(acac)$ dye in the film (Figure 7). At 80 K in the mixed dye PS film, the rise time amounts to 51 ns (Table 1), in fair agreement with the inverse energy transfer rate $k_q^{-1} = 40$ ns determined from the photoluminescence lifetime quenching of the Ir(*t*Bu-ppy)$_3$ dye. The quantitative correspondence of the characteristic time constants of the two processes strongly suggests a mutual origin, consistent with triplet energy transfer from Ir(*t*Bu-ppy)$_3$ to $Ir(btp)_2(acac)$.

In thin films at 80 K, diffusion of molecules can be excluded and an energy transfer mechanism that involves diffusion via the triplet state the PS matrix is highly unlikely. The fact that the energy transfer is very efficient in the mixed films seems to indicate that a Förster mechanism is operative, but—at this stage—the Dexter mechanism cannot be fully excluded because the relatively high concentration (90−100 mM; 6−7 wt %) of the dyes give rise to an average distance between the dyes that does not preclude some orbital overlap. The radius $R_c$ of the average spherical volume available to a phosphorescent dye molecule at molar concentration $C$ is $R_c = [3/(4\pi N_A C)]^{1/3}$ and equals $R_c = 1.6$ nm at $C = 100$ mM. This can be compared to the radius of the molecule as determined from the molecular volume provided by the crystallographic structure. For the related $Ir(ppy)_3$ and $Ir(ppy)_2(acac)$ complexes this radius is 0.51−0.53 nm and of the same order of magnitude as $R_c$.[43,44] In the next section it will be shown, however, that the Dexter mechanism can be excluded as being the major process.

**Energy Transfer between Ir(*t*Bu-ppy)$_3$ and 3T in Solution.** To differentiate between the Dexter and Förster mechanisms, it is possible to use a molecule that has a triplet state lower than that of Ir(*t*Bu-ppy)$_3$ but which has a negligible absorption coefficient for the $T_1 \leftarrow S_0$ absorption. When the transition dipole moment is extremely small, the Förster mechanism cannot be operative and energy transfer can only occur via direct exchange and orbital overlap. From previous experiments and quantum chemical calculations, terthiophene (3T) is known to have the desired properties for this experiment (Figure 8).[45] The first triplet state of 3T is at 689 nm (1.80 eV, i.e., well below the phosphorescent $^3$MLCT state of the Ir(*t*Bu-ppy)$_3$ at 2.41 eV), and it is has negligible absorption below the onset of the $S_1 \leftarrow S_0$ absorption at 410 nm (3.0 eV).

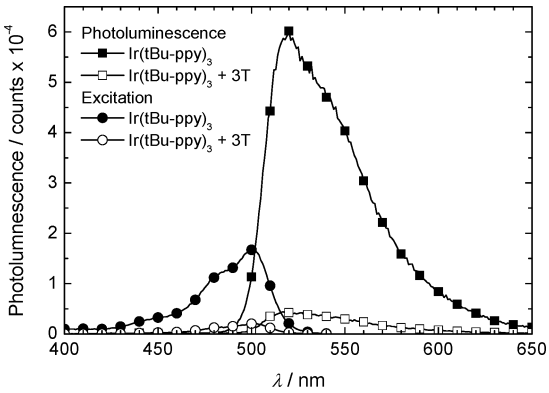


**Figure 9.** Photoluminescence (squares) and excitation (circles) spectra of Ir(*t*Bu-ppy)$_3$ (1 mM) (solid symbols) and of a mixture of Ir(*t*Bu-ppy)$_3$ (1 mM) and 3T (1 mM) (open symbols) in MeTHF solution. Photoluminescence was recorded using an excitation wavelength of 400 nm. Excitation spectra were recorded at 550 nm. All experiments were performed under inert atmosphere at room temperature.

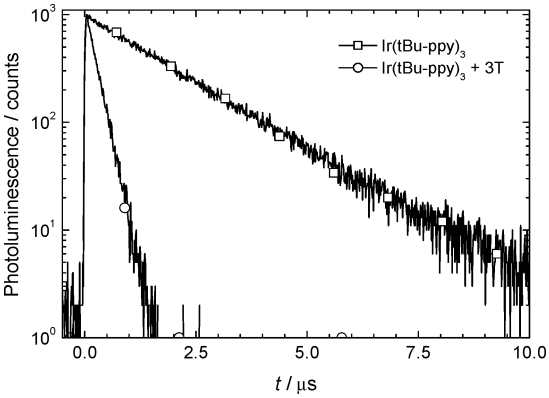


**Figure 10.** Time-resolved photoluminescence recorded at 535 nm of Ir(*t*Bu-ppy)$_3$ in MeTHF (squares) and of Ir(*t*Bu-ppy)$_3$ (1 mM) mixed with 3T (1 mM) (circles). The photoluminescence was recorded under inert atmosphere at room temperature with pulsed excitation at 400 nm.

Photoluminescence quenching experiments of Ir(*t*Bu-ppy)$_3$ mixed with 3T have been performed at room temperature under inert atmosphere in MeTHF solution. The photoluminescence and excitation spectra reveal significant quenching of the emission of the Ir(*t*Bu-ppy)$_3$ emission upon addition of 3T (Figure 9). The intensity of the emission at 535 nm is quenched by $Q = 8$ as determined from the excitation spectra at 500 nm. The quenching factor determined from the photoluminescence spectra in Figure 9 seems larger ($Q = 13$), but the absorption of 3T at the excitation wavelength of 400 nm causes this number to be overestimated.

The time-resolved photoluminescence of Ir(*t*Bu-ppy)$_3$ with and without 3T (Figure 10) confirms that addition of 3T quenches the excited state of Ir(*t*Bu-ppy)$_3$. The lifetime of the Ir(*t*Bu-ppy)$_3$ luminescence decreases from 1.73 $\mu$s to 229 ns upon addition of 3T (Table 1). The pseudo-first-order rate constant for quenching via energy transfer under these conditions determined from the lifetime, $k_q = \tau_Q^{-1} - \tau_0^{-1} = 3.8 \times 10^6\ s^{-1}$, is in excellent agreement with the rate, $k_q = (Q - 1)/\tau_0 = 4.0 \times 10^6\ s^{-1}$, determined from the 8-fold photoluminescence quenching with excitation at 500 nm. With the use of the lifetime quenching and the concentration of the quencher, the second-order rate constant for energy transfer is then $k_{en} = 3.8 \times 10^9$ L mol$^{-1}$ s$^{-1}$. The diffusion constant for MeTHF ($\eta = 0.5618 \times 10^{-3}$ Pa·s)[46] at 298 K was calculated as $k_{diff} = 1.2 \times 10^{10}$ L mol$^{-1}$ s$^{-1}$.

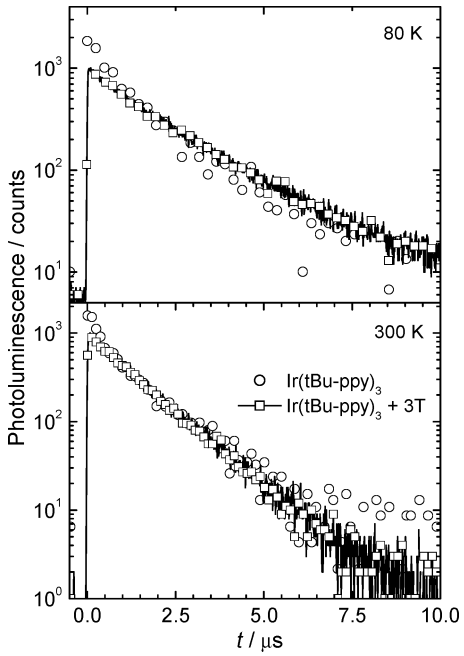


**Figure 11.** Time-resolved photoluminescence of PS films containing 8 wt % (100 mM) Ir(*t*Bu-ppy)$_3$ recorded at 535 nm (squares) and containing a mix of 8 wt % (100 mM) Ir(*t*Bu-ppy)$_3$ and 5 wt % (210 mM) 3T recorded at 535 nm (circles). The photoluminescence was recorded under inert atmosphere at 80 and 300 K with pulsed excitation at 400 nm.

The steady-state and time-resolved photoluminescence experiments show that in solution triplet energy transfer from Ir(*t*Bu-ppy)$_3$ to the low-energy (1.80 eV) triplet state of 3T occurs via a diffusion-controlled mechanism. The negligible absorption coefficient of 3T in the wavelength range where Ir(*t*Bu-ppy)$_3$ emits precludes that Förster energy transfer is involved, and hence, the quenching is attributed to Dexter exchange.

**Absence of Energy Transfer between Ir(*t*Bu-ppy)$_3$ and 3T in Thin Films.** The time-resolved photoluminescence of the phosphorescent Ir(*t*Bu-ppy)$_3$ dye in thin PS films with and without 3T as a quencher have been recorded at 80 and 300 K (Figure 11). The temporal evolution of the emission of Ir(*t*Bu-ppy)$_3$ with and without 3T is virtually identical, and the lifetimes of Ir(*t*Bu-ppy)$_3$ without (2.07 $\mu$s) and with 3T (1.91 $\mu$s) (Table 1) lie within sample-to-sample variations. This shows that 3T does not quench the $^3$MLCT state of Ir(*t*Bu-ppy)$_3$ in the solid PS matrix. The only noticeable difference in Figure 11 is the presence of a fast component at short times after excitation for the mixed Ir(*t*Bu-ppy)$_3$ + 3T film which is absent in the film without 3T. This fast component is due to a contribution of the short-lived fluorescence of 3T that is also excited at 400 nm. While the intensity of the steady-state photoluminescence spectra recorded at 80 K show distinct sample-to-sample variations, there was no consistent effect of the addition of 3T on the photoluminescence intensity of Ir(*t*Bu-ppy)$_3$, corroborating that energy transfer from the $^3$MLCT state of Ir(*t*Bu-ppy)$_3$ to 3T is absent under these conditions. The fact that at higher temperature (300 K) the results for the two films are also identical indicates that diffusion of triplet excitons toward 3T molecules is negligible.

**Förster Energy Transfer in Thin Films.** Comparison of the quenching experiments of Ir(*t*Bu-ppy)$_3$ in PS at 80 K using the absorbing and phosphorescent Ir(btp)$_2$(acac) dye (i.e., with a nonzero oscillator strength) or the nonabsorbing nonemissive 3T molecule clearly shows that Ir(btp)$_2$(acac) quenches the excited state of Ir(*t*Bu-ppy)$_3$ far more efficiently than 3T. Since all conditions and parameters such as temperature, matrix, quencher concentration are comparable for the two experiments, the difference in quenching efficiency must be due to the characteristics of the quencher. On the basis of the properties of the quencher it is now possible to differentiate between the Förster and Dexter mechanisms.

In terms of a Förster mechanism, 3T is a poor quencher due to the extremely low, essentially zero, oscillator strength of the $T_1 \leftarrow S_0$ transition. In contrast, Ir(btp)$_2$(acac) is a much better quencher because it has significant absorption in the wavelength range where Ir(*t*Bu-ppy)$_3$ emits, and hence the transition to the ligand-based $^3(\pi-\pi^*)$ has a nonzero oscillator strength. In Dexter transfer the oscillator strengths are not important, and 3T and Ir(btp)$_2$(acac) would give similar quenching. The much stronger quenching of Ir(*t*Bu-ppy)$_3$ by Ir(btp)$_2$(acac) compared to that of 3T in thin films indicates that Förster triplet energy transfer is the dominant mechanism under these conditions.

To quantify the results it is possible to determine the Förster radius $R_0$:

$$R_0^{\,6} = \frac{9000\kappa^2 \ln(10)\phi}{125\pi^5 n^4 N_A} \frac{\int I_D(\lambda)\epsilon_A(\lambda)\lambda^4 \, d\lambda}{\int I_D(\lambda) \, d\lambda} \qquad (1)$$

where$\lambda$ is the wavelength, $\kappa^2$ is an orientation factor that equals $^2/_3$ for an isotropic sample, $\phi = 0.56 \pm 0.04$ is the luminescence quantum yield of the donor, $I_D(\lambda)$ is the emission of the donor, $\epsilon_A(\lambda)$ is the molar absorption of the acceptor, $n$ is the refractive index of the solvent in which absorption and luminescence were recorded, and $N_A$ is Avogadro's constant. The Förster radius for energy transfer between the green Ir(*t*Bu-ppy)$_3$ dye and the red Ir(btp)$_2$(acac) dye amounts to $R_0 = 3.02$ nm. This can be used to estimate the photoluminescence quenching of Ir(*t*Bu-ppy)$_3$ in a solid PS matrix with Ir(btp)$_2$(acac) as an acceptor. For Förster energy transfer from a donor to an acceptor that is randomly distributed in three dimensions, with slow translational diffusion compared to the rate of transfer, the luminescence quenching amounts to[47]

$$\frac{1}{Q} = 1 - \sqrt{\pi}\gamma \exp(\gamma^2)[1 - \mathrm{erf}(\gamma)] \qquad (2)$$

where $\gamma$ is given by

$$\gamma = \frac{\sqrt{\pi}}{2} C_A \frac{4}{3} \pi R_0^{\,3} \qquad (3)$$

with $C_A$ the concentration of acceptors (number per nm$^3$). In Figure 12 the quenching constant $Q$ is plotted as function of $R_0$. The experimental results $Q = 63$ (from lifetime experiments) and $Q = 62$ (from steady-state quenching experiments) are accurately reproduced by eq 2 at the Förster radius $R_0 \approx 3.02$ nm, where $Q = 64$. This quantitative agreement provides further evidence that in the mixed films triplet Förster energy transfer occurs.

## Conclusion

Photoluminescence quenching of the green phosphorescent emitter Ir(*t*Bu-ppy)$_3$ has been investigated in solution and in an inert PS matrix using the red phosphorescent Ir(btp)$_2$(acac) dye and 3T molecule that has a low-energy $^3(\pi-\pi^*)$state. Both Ir(btp)$_2$(acac) (2.00 eV) and 3T (1.80 eV) have a triplet state energy that is lower than that of Ir(*t*Bu-ppy)$_3$ (2.41 eV), implying that energy transfer can occur for both molecules. The two quenchers differ strongly, however, in their absorption coef-

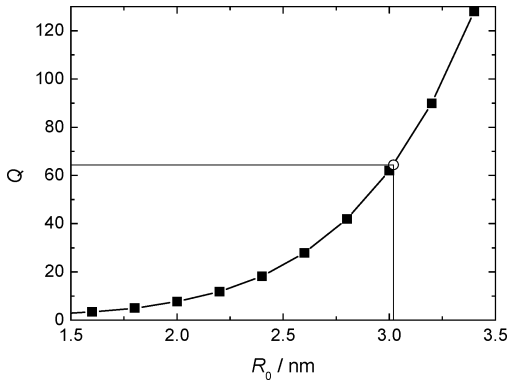


**Figure 12.** Quenching factor $Q$ as function of the Förster radius $R_0$ calculated from eq 2 and an acceptor concentration of 90 mM. The open circle gives the experimental result for $R_0 = 3.02$ nm.

ficient in the wavelength region where the Ir(*t*Bu-ppy)$_3$ emits (500−650 nm). Here, Ir(btp)$_2$(acac) has a low, but distinct, absorption, while that of 3T is essentially zero. As a consequence Ir(btp)$_2$(acac) can participate in both Förster and Dexter triplet energy transfer, while for 3T only the Dexter mechanism is possible.

In solution, both molecules quench the photoluminescence of Ir(*t*Bu-ppy)$_3$ via triplet energy transfer with second-order rate constant $k_{en} = 3.8 \times 10^9$ L mol$^{-1}$ s$^{-1}$, indicating that the energy transfer is diffusion limited. In a PS matrix, on the other hand, the transfer efficiency for Ir(btp)$_2$(acac) and 3T differs dramatically. Under similar conditions, the phosphorescent Ir(btp)$_2$(acac) dye (6 wt %, 90 mM) quenches the Ir(*t*Bu-ppy)$_3$ emission by almost 2 orders of magnitude, while 3T (5 wt %, 210 mM) shows hardly any quenching.

The energy transfer mechanisms that operate in solution and in the PS matrix are different. In solution, where molecular diffusion is possible, the energy transfer is diffusion controlled, with a rate constant that is independent of the nature of the quencher. The actual quenching mechanism in solution for 3T must be a Dexter transfer, relying on orbital overlap in the deactivation step, but for Ir(btp)$_2$(acac) the energy transfer can take place via both Förster and Dexter mechanisms.

Molecular diffusion can be neglected in thin PS films at 80 K, and hence triplet energy transfer can only occur via the Förster mechanism. This point of view is strongly supported by the experimental result that effective quenching only occurs for Ir(btp)$_2$(acac) and not for 3T in PS, as expected for Förster transfer considering the much higher transition dipole moment of Ir(btp)$_2$(acac) compared to that of 3T. Moreover, a model for luminescence quenching via Förster energy transfer from a donor to acceptor molecules that are randomly distributed in three dimensions in a rigid matrix (eq 2) provides quantitative agreement with the experimental phosphorescence quenching in the films when using the Förster radius ($R_0 = 3.02$ nm) of the two iridium complexes determined from the photophysical data. Hence, the Förster mechanism is the prevailing mechanism for phosphorescent resonant energy transfer under these conditions.

The result that in a rigid polymer matrix triplet energy transfer between different phosphorescent dopants occurs via the Förster mechanism may be used to rationally tune the emission spectra of mixed layers[31] toward more optimal white-light emission.

## Experimental Section

The synthesis of the green-emitting Ir(*t*Bu-ppy)$_3$ dye[35] and 3T[48] have been performed according to published methods. The red-emitting Ir(btp)$_2$(acac) dye (American Dye Source) and polystyrene ($M_w = 250$ kDa) were used as received. Anhydrous, sealed chlorobenzene (Aldrich) was used as received and kept under inert atmosphere at all times. 2-Methyltetrahydrofuran (MeTHF) was predried over KOH for 3 days, filtered, distilled from $CaH_2$, and stored under inert nitrogen atmosphere.

Sample solutions were prepared in a nitrogen glove box using dry and deoxygenated MeTHF or chlorobenzene. Thin film samples were spin coated at 1100 rpm using an Electronic Micro Systems' photo resist spinner (model 4000) inside a glove box. The polymer solutions used for spin coating were prepared in the glove box by stirring overnight and heating to 70 °C for 1 h, after which the films were spin coated. Film thickness was determined using a Tencor P-10 surface profilometer.

UV−vis and photoluminescence spectra were recorded using a Perkin-Elmer Lambda 900 and an Edinburgh Instruments FS920 spectrophotometer, respectively. Time-correlated single-photon counting (TCSPC) photoluminescence was performed on an Edinburgh Instruments LifeSpec-PS spectrometer by photoexcitation at 400 nm with a picosecond-pulse laser (PicoQuant PDL 800B) operated at 2.5 MHz, 400 kHz, or 40 kHz and using a Peltier-cooled Hamamatsu microchannel plate photomultiplier (R3809U-50) for detection. During the spectroscopic experiments, thin film samples were held at 80 or 300 K under nitrogen atmosphere using an Oxford Optistat CF continuous flow cryostat or an Oxford Optistat DN bath cryostat. All solutions were kept under inert atmosphere. The quantum yield of Ir(*t*Bu-ppy)$_3$ was determined using *N*,*N*′-bis(1-ethylpropyl)perylenediimide ($\phi = 1$) as a standard. The excitation wavelength was 480 nm, and both samples had similar OD (<0.1). The integrated emission spectra were corrected by dividing by the number of absorbed photons.

**Acknowledgment.** We thank Bea Langeveld, Jolanda Bastiaansen, and Nicole Kiggen (TNO Science and Industry) for a generous gift of Ir(*t*Bu-ppy)$_3$ and experimental assistance in the preparation of films. The research was supported by The Netherlands Organization for Scientific Research (NWO) through a grant in the PIONIER program and by the Interreg program OLED$^+$.

## References and Notes

(1) Tang, C. W.; VanSlyke, S. A. *Appl. Phys. Lett.* **1987**, *51*, 913.
(2) Burroughes, J. H.; Bradley, D. D. C.; Brown, A. R.; Marks, R. N.; Mackay, K.; Friend, R. H.; Burns, P. L.; Holmes, A. B. *Nature* **1990**, *347*, 539.
(3) Kido, J.; Kimura, M.; Nagai, K. *Science* **1995**, *267*, 1332.
(4) Kido, J.; Nagai, K.; Ohashi, Y. *Chem. Lett.* **1990**, 657.
(5) Baldo, M. A.; O'Brien, D. F.; You, Y.; Shoustikov, A.; Sibley, S.; Thompson, M. E.; Forrest, S. R. *Nature* **1998**, *395*, 151.
(6) O'Brien, D. F.; Baldo, M. A.; Thompson, M. E.; Forrest, S. R. *Appl. Phys. Lett.* **1999**, *74*, 442.
(7) Baldo, M. A.; Lamansky, S.; Burrows, P. E.; Thompson, M. E.; Forrest, S. R. *Appl. Phys. Lett.* **1999**, *75*, 4.
(8) Adachi, C.; Baldo, M. A.; Forrest, S. R.; Lamansky, S.; Thompson, M. E.; Kwong, R. C. *Appl. Phys. Lett.* **2001**, *78*, 1622.
(9) Holmes, R. J.; D'Andrade, B. W; Forrest, S. R.; Ren, X.; Li, J.; Thompson, M. E. *Appl. Phys. Lett.* **2003**, *83*, 3818.
(10) Lee, C. L.; Lee, K. B.; Kim, J. J. *Appl. Phys. Lett.* **2000**, *77*, 2280.
(11) Wilson, J. S.; Dhoot, A. S.; Seeley, A. J. A. B.; Khan, M. S.; Köhler, A.; Friend, R. H. *Nature* **2001**, *413*, 828.
(12) Gong, X.; Robinson, M. R.; Ostrowski, J. C.; Moses, D.; Bazan, G. C.; Heeger, A. J. *Adv. Mater.* **2002**, *14*, 581.
(13) Zhu, W.; Mo, Y.; Yuan, M.; Yang, W.; Cao, Y. *Appl. Phys. Lett.* **2002**, *80*, 2045.
(14) Gong, X.; Ostrowski, J. C.; Bazan, G. C.; Mozes, D.; Heeger, A. J.; Liu, M. S.; Jen, A. K. Y. *Adv. Mater.* **2003**, *15*, 45.
(15) Sandee, A. J.; Williams, C. K.; Evans, N. R.; Davies, J. E.; Boothby, C. E.; Köhler, A.; Friend, R. H.; Holmes, A. B. *J. Am. Chem. Soc.* **2004**, *126*, 7041.

(16) Adachi, C.; Baldo, M. A.; Thompson, M. E.; Forrest, S. R. *J. Appl. Phys.* **2001**, *90*, 5048.

(17) Baldo, M. A.; Forrest, S. R. *Phys. Rev. B* **2000**, *62*, 10958.

(18) Baldo, M. A.; Adachi, C.; Forrest, S. R. *Phys. Rev. B* **2000**, *62*, 10967.

(19) Gong, X.; Ostrowski, J. C.; Moses, D.; Bazan, G. C.; Heeger, A. J. *Adv. Funct. Mater.* **2003**, *13*, 439.

(20) Gong, X.; Lim, S. H.; Ostrowski, J. C.; Mozes, D.; Bardeen, C. J.; Bazan, G. C. *J. Appl. Phys.* **2004**, *95*, 948.

(21) Brunner, K.; van Dijken, A.; Börner, H.; Bastiaansen, J. J. A. M.; Kiggen, N. M. M.; Langeveld, B. M. W. *J. Am. Chem. Soc.* **2004**, *126*, 6035.

(22) Evans, N. R.; Sudha Devi, L.; Mak, C. S. K.; Watkins, S. E.; Pascu, S. I.; Köhler, A.; Friend, R. H.; Williams, C. K.; Holmes, A. B. *J. Am. Chem. Soc.* **2006**, *128*, 6647.

(23) D'Andrade, B. W.; Thompson, M. E.; Forrest, S. R. *Adv. Mater.* **2002**, *14*, 147.

(24) Adamovich, V.; Brooks, J.; Tamayo, A.; Alexander, A. M.; Djurovich, P. I.; D'Andrade, B. W.; Adachi, C.; Forrest, S. R.; Thompson, M. E. *New J. Chem.* **2002**, *26*, 1171.

(25) D'Andrade, B. W.; Forrest, S. R. *Adv. Mater.* **2004**, *16*, 1585.

(26) Gong, X.; Ma, W.; Ostrowski, J. C.; Bazan, G. C.; Moses, D.; Heeger, A. J. *Adv. Mater.* **2004**, *16*, 615.

(27) Gong, X.; Wang, S.; Mozes, D.; Bazan, G. C.; Heeger, A. J. *Adv. Mater.* **2005**, *17*, 2035.

(28) Sun, Y.; Giebink, N. C.; Kanno, H.; Ma, B.; Thompson, M. E.; Forrest, S. R. *Nature* **2006**, *440*, 908.

(29) Baldo, M. A.; Thompson, M. E.; Forrest, S. R. *Nature* **2000**, *403*, 750.

(30) D'Andrade, B. W.; Baldo, M. A.; Adachi, C.; Brooks, J.; Thompson, M. E.; Forrest, S. R. *Appl. Phys. Lett.* **2001**, *79*, 1045.

(31) D'Andrade, B. W.; Holmes, R. J.; Forrest, S. R. *Adv. Mater.* **2004**, *16*, 624.

(32) Kawamura, Y.; Brooks, J.; Brown, J. J.; Sasabe, H.; Adachi, C. *Phys. Rev. Lett.* **2006**, *96*, 017404.

(33) Colombo, M. G.; Brunold, T. C.; Riedener, T.; Güdel, H. U.; Förtsch, M.; Bürgi, H. B. *Inorg. Chem.* **1994**, *33*, 545.

(34) Dedian, K.; Djurovich, P. I.; Garces, F. O.; Carlson, G.; Watts, R. J. *Inorg. Chem.* **1991**, *30*, 1685.

(35) Zhu, W.; Liu, C.; Su, L.; Yang, W.; Yuan, M.; Cao, Y. *J. Mater. Chem.* **2003**, *13*, 50.

(36) King, K. A.; Spellane, P. J.; Watts, R. J. *J. Am. Chem. Soc.* **1985**, *107*, 1431.

(37) Kawamura, Y.; Goushi, K.; Brooks, J.; Brown, J. J.; Sasabe, H.; Adachi, C. *Appl. Phys. Lett.* **2005**, *86*, 071104.

(38) Lamansky, S.; Djurovich, P.; Murphy, D.; Abdel-Raazaq, F.; Lee, H. E.; Adachi, C.; Burrows, P. E.; Forrest, S. R.; Thompson, M. E. *J. Am. Chem. Soc.* **2001**, *123*, 4304.

(39) Tsuboyama, A.; Iwawaki, H.; Furogori, M.; Mukaide, T.; Kamatani, J.; Igawa, S.; Moriyama, T.; Miura, S.; Takiguchi, T.; Okada, S.; Hoshino, M.; Ueno, K. *J. Am. Chem. Soc.* **2003**, *125*, 12971.

(40) At an excitation wavelength of 500 nm and the concentrations used [10 mM Ir(*t*Bu-ppy)$_3$ and 550 $\mu$M Ir(btp)$_2$(acac)] the absorbance of Ir(*t*Bu-ppy)$_3$ and Ir(btp)$_2$(acac) in a 1 cm cell is 12.3 and 3.9, respectively. Figure 3 shows that the major emission in the mixture is from the red-emitting dye, while most light is absorbed by the green-emitting dye. The curve for 100% energy transfer in the mixture is the emission of an optically dense Ir(btp)$_2$(acac) solution. The curve for 0% energy transfer in the mixture assumes that only light absorbed by Ir(btp)$_2$(acac) itself leads to emission. In the mixture this fraction is 3.9/(12.3 + 3.9) of the intensity of a pure and optically dense sample of Ir(btp)$_2$(acac).

(41) Debye, P. *Trans. Electrochem. Soc.* **1942**, *82*, 265.

(42) Singh, R. P.; Sinha, C. P. *J. Chem. Eng. Data* **1985**, *30*, 470.

(43) Breu, J.; Stoessel, P.; Schrader, S.; Starukhin, A.; Finkenzeller, W. J.; Yersin, H. *Chem. Mater.* **2005**, *17*, 1745.

(44) Lamansky, S.; Djurovich, P.; Murphy, D.; Abdel-Raazaq, F.; Kwong, R.; Tsyba, I.; Bortz, M.; Mui, B.; Bau, R.; Thompson, M. E. *Inorg. Chem.* **2001**, *40*, 1704.

(45) Wasserberg, D.; Marsal, P.; Meskers, S. C. J.; Janssen, R. A. J.; Beljonne, D. *J. Phys. Chem. B* **2005**, *109*, 4410.

(46) Vallés, C.; Pérez, E.; Mainar, A. M.; Santafé, J.; Domínguez, M. *J. Chem. Eng. Data* **2006**, *51*, 1105.

(47) Valeur, B. *Molecular Fluorescence: Principles and Applications*; Wiley-VCH: Weinheim, Germany, 2002.

(48) Wynberg, H.; Metselaar, J. *Synth. Commun.* **1984**, *14*, 1.